J Prosthodont Res. 2022; **(**): ****–****

OPEN ACCESS JPR Journal of Prosthodontic Research Original article

Mechanical and surface properties of additive manufactured zirconia under the different building directions

Shoko Miura [a,*], Akikazu Shinya [b,c], Yoshiki Ishida [b], Masanori Fujisawa [a]

[a] Division of Fixed Prosthodontics, Department of Restorative & Biomaterials Sciences, Meikai University School of Dentistry, Japan

[b] Department of Dental Materials Sciences, School of Life Dentistry at Tokyo, The Nippon Dental University, Japan

[c] Department of Prosthetic Dentistry and Biomaterials Science, Institute of Dentistry, University of Turku, Finland

Abstract

Purpose: This study investigates the mechanical and surface properties of zirconia manufactured using additive manufacturing (AM) technology and the effect of the building direction on the mechanical and surface properties.

Methods: Specimens were prepared using ZrO_2 paste (3DMix ZrO_2; 3DCeram) and a three-dimensional printing system (CeraMaker 900; 3DCeram) based on the principles of stereolithography (SLA). The mechanical properties (flexural strength, Vickers hardness, fracture toughness, elastic modulus, and Poisson's ratio) and surface properties (chemical composition and surface observation) were evaluated for three building directions (parallel, diagonal, and perpendicular) to investigate the relationship between the building directions and the anisotropy of the mechanical and surface properties of SLA-manufactured zirconia. Statistical analysis was performed using a one-way analysis of variance and Tukey's honestly significant difference test.

Results: The highest flexural strength was obtained for a perpendicular building direction. The flexural strength was significantly higher in the perpendicular direction than in the parallel and diagonal directions; it was also significantly higher in the diagonal direction than in the parallel direction ($p<0.05$). The Vickers hardness, fracture toughness, elastic modulus, Poisson's ratio, and chemical composition did not differ significantly. Microstructural observations revealed that the layers, large crystals, and pores were more prominent in the parallel direction.

Conclusions: The flexural strength and surface structure of the tested SLA-manufactured zirconia were influenced by the building direction; however, other mechanical properties remained unaffected. The layer boundaries affected the anisotropic behavior of the builds to a certain extent, owing to the layer-by-layer production method.

Keywords: Anisotropy, Digital dentistry, Material properties, Y-TZP, 3D printing

Received 9 June 2022, Accepted 12 October 2022, Available online 19 November 2022

1. Introduction

The clinical application of dental prostheses manufactured using dental computer-aided design/computer-aided manufacturing (CAD/CAM) systems is now common, owing to the advances in digitalization in the field of dentistry[1]. A CAD/CAM system includes the processes of designing a dental prosthesis using CAD software, converting the scanned data into machining data using CAM software, and using either subtractive manufacturing (SM) or additive manufacturing (AM) technologies to fabricate the dental prosthesis. The former method is employed to fabricate dental prostheses that involve the milling of block- or disk-shaped materials using milling tools[2]. However, SM technologies generate a significant amount of waste materials and tools, and their production of parts with complex geometries is limited, owing to the milling tool size[3]. Previous studies on SM technologies have reported that they are highly reliable, as evidenced by their widespread use in the field of prosthetic dentistry[4–7]. In particular, zirconia ceramics can only be used to fabricate dental prostheses with a CAD/CAM system, and SM technologies are considered state-of-the-art for fabricating all-ceramic restorations containing zirconia ceramics[8,9]. Zirconia ceramics exhibit exceptional mechanical properties (such as strength, hardness, fracture toughness, wear resistance, corrosion resistance, and biocompatibility) and offer ease of machining through SM technologies in the pre-sintering stage[10–12]. However, manufacturing objects with complex geometries is challenging, owing to the limitations associated with milling tools, such as their size and applied angle[13]. In contrast, AM technologies enable the build-up of pieces by adding the material layer-by-layer, unlike SM technologies, which are based on a computerized three-dimensional (3D) printing model. Furthermore, AM technologies can be used to create dental restorations with near-net-shaped dental prostheses that feature intricate details (i.e., grooves, crannies, and valleys), which cannot be fabricated using SM technologies[14,15].

The American Society of Testing and Materials has classified

DOI: https://doi.org/10.2186/jpr.JPR_D_22_00166

***Corresponding author:** Shoko Miura, Division of Fixed Prosthodontics, Department of Restorative & Biomaterials Sciences, Meikai University School of Dentistry, 1-1 Keyakidai, Sakado, Saitama, 350-0248, Japan.

E-mail address: miuras@dent.meikai.ac.jp

seven different AM technologies: vat photopolymerization, material jetting, material extrusion or fused deposition modeling, binder jetting, powder bed fusion (PBF), sheet lamination, and direct energy deposition[16]. The earliest application of dental materials that can be used in AM technologies was the medical modeling of surgical guides using polymers[15,17,18]. This recent and novel technology has gained increased interest and clinical applications in dentistry, owing to the wide range of features that allow it to provide interim restorations, occlusal splints, bite guards, scaffolds, and orthodontic appliances[15,19,20]. Other materials have also been utilized for the production of dental prostheses using the cobalt–chrome PBF bonding method, the fabrication of metal frames such as porcelain-fused-to-metal crowns, and metal denture bases and clasps[21–23]. In addition, the combination of AM technologies with materials suitable for dental applications enabled the integration of digital workflows in dentistry, thereby adopting AM technologies for the production of resins and metal dental prostheses[3,14,21,24–27]. Furthermore, unlike SM technologies, AM technologies result in less material waste and energy consumption. In addition, they eliminate the use of conventional milling tools[15]. Therefore, they are more feasible because they reduce the consumption of raw materials[15]. With the development of AM technologies, stereolithographic techniques, such as stereolithography (SLA) and digital light processing (DLP), have shown promising results for the fabrication of zirconia-based dental prostheses[28,29]. These techniques are used to achieve the layer-by-layer printing of 3D objects by enabling the light-curing process for resins in a ceramic paste. This is followed by post-treatments, such as the de-binding and sintering steps, which are required to remove the organic resin and generate a dense material[30]. Moreover, these technologies enable rapid printing and allow the manufacture of complex geometries with high accuracy and excellent surface quality[15]. However, the commercialization of AM technologies for the production of ceramic crowns remains in its infancy and has limited clinical applicability[31]. Literature on the use of zirconia in AM technologies has recently increased. However, to date, only a few studies have compared the mechanical properties and accuracy of zirconia specimens manufactured using SM and AM technologies[3,28,30,32]. Recent studies have also raised concerns that ceramic additive-manufactured parts exhibit strong anisotropy in terms of the mechanical properties associated with building directions[33,34]. However, the effect of the building direction on the mechanical properties of additive-manufactured zirconia specimens has not yet been fully investigated. Therefore, it is important to understand the relationship between the building direction and mechanical and surface properties and how it may cause this anisotropy when designing additive-manufactured dental prostheses to ensure their safe use. Thus, this study aims to clarify the effect of the building direction on the mechanical and surface properties of additive-manufactured zirconia specimens. The null hypothesis is that the mechanical properties of additive-manufactured zirconia materials do not differ significantly based on the building direction.

2. Materials and methods

In this study, the flexural strength, Vickers hardness, fracture toughness, elastic modulus, Poisson's ratio, chemical composition, and surface structure of partially stabilized SLA-manufactured zirconia were characterized according to applicable standards. This characterization was performed for three different building directions to investigate the relationship between the building direction and the anisotropy of the mechanical and surface properties of SLA-manufactured zirconia specimens. The positioning data of the specimens were set parallel (0°), diagonal (45°), and perpendicular (90°) to the building direction **(Fig. 1**). For the elastic modulus and Poisson's ratio, in the 90° direction, an X-axis horizontal to the building stage (90°-x) and a Y-axis perpendicular to the building direction (90°-y) were specified for the specimens.

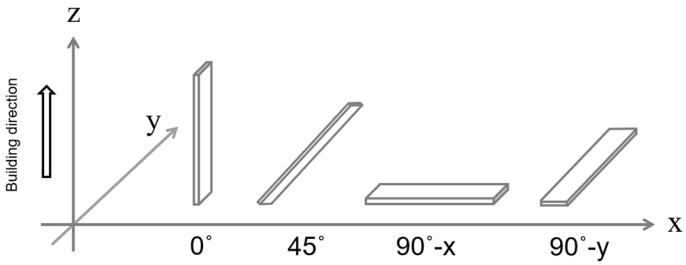

Fig. 1. Building directions of additive-manufactured zirconia specimens. The specimens were set parallel (0°), diagonal (45°), and perpendicular (90°) to the building direction. In the 90° building direction, an X-axis horizontal to the building stage (90°-x) and a Y-axis perpendicular to the building direction (90°-y) were specified in the specimens.

Table 1. Material used in this study

Material	Manufacturer	Composition	Lot No.
3DMix ZrO_2	3DCeram	Zirconia stabilized with 3 mol% yttria	ZRJ004-19

2.1. Specimen preparation

The digital design of the bar specimens was created using open-source software (3D Builder, v.18.0.1931.0, Microsoft, Redmond, WA, USA) and saved as a standard tesselation language (STL) file. The specimens were prepared using a ZrO_2 (zirconia stabilized with 3 mol% yttria) paste of a dedicated material (3DMix ZrO_2; 3DCeram, Limoges, France) (**Table 1**) and 3D printing system using the vat photopolymerization method for an AM device (CeraMaker 900; 3DCeram). SLA is based on the dimensionally controlled polymerization of a photosensitive-resin-coated ceramic slurry contained in a vat. A computer-controlled laser beam was used to illuminate the slurry surface in a pattern dictated by the shape of the object[35]. Consequently, the first layer of the illuminated resin solidified and adhered to the built platform[31]. In the SLA process, the laser source was positioned above the vat, and the parts were fabricated facing upward. The building platform was immersed in a vat and positioned immediately below the resin surface. Only a thin resin layer with a specific thickness was exposed to the laser source above. Once a layer was cured, the building platform moved downward along the Z-axis by the thickness of one layer to spread a fresh resin layer on top of the previously cured layer[36]. The platform movement and curing of an individual pattern in a resin layer were repeated to construct a solid 3D object. After printing, the de-binding process was performed by placing the green parts in a de-binding furnace to remove the organic parts and wash off the excess resin. The resulting ZrO_2 was solvent-degreased, dried, and sintered[15,29]. ZrO_2 was sintered in a furnace at approximately 1,500 °C. The details of the sintering process are proprietary information provided by the manufacturer. Because ZrO_2 shrinks by approximately 20% after sintering, the specimens were designed to account for the dimensional changes after sintering. All the specimens were fabricated by the manufacturer.

2.2. Flexural strength measurement

The testing method was in accordance with ISO standard (6872:2015)[37]. The specimens were prepared according to dimensions of 1.2 × 4.0 × 25.0 mm with #400 water-resistant abrasive paper (Struers, Copenhagen, Denmark), and they were polished with #800 water-resistant abrasive paper (Struers) (n = 10). The fabricated specimens were immersed in ultrapure water (Milli-Q Reference, Merck, Burlington, MA, USA) at 37 °C for 24 h. A three-point bending test was conducted using a universal testing machine (AGS-X, Shimadzu, Kyoto, Japan) at a crosshead speed of 1.0 mm/min. The flexural strength σ (MPa) is expressed as follows:

$$\sigma = 3PL/2wt^2,$$

where P is the load at failure; L is the distance between the supports, which is equal to 20 mm; and w and t are the pre-measurement specimen width and thickness, respectively.

2.3. Vickers hardness and fracture toughness measurement

The specimen dimensions were 10 × 10 × 3 mm with #400 water-resistant abrasive paper (Struers), and it was polished with #800 water-resistant abrasive paper (Struers). The specimens were immersed in ultrapure water at 37 °C for 24 h. An experiment was conducted using the indentation-fracture method with a Vickers hardness tester (AK-15, Akashi, Tokyo, Japan). The Vickers indenter was pressed onto the test specimen to generate semicircular or semielliptical vertical cracks around the indentation. The lengths of these cracks were measured, and the fracture toughness ($MPam^{1/2}$) was calculated for the measured value using Niihara's formula[38], as follows:

$$K_{IC} = 0.203(c/a)^{-3/2}Ha^{1/2},$$

where K_{IC} is the fracture toughness ($MPam^{1/2}$), a is 1/2 of the indentation diagonal length (μm), c is 1/2 of the crack length (μm), and H is the Vickers hardness. The Vickers hardness was measured under a measurement load of 20 kg (196 N) and load holding time of 10 s.

2.4. Elastic modulus and Poisson's ratio measurement

The specimen dimensions were prepared to 1.2 × 4.0 × 25.0 mm with #400 water-resistant abrasive paper (Struers), and the specimen was polished with #800 water-resistant abrasive paper (Struers). An orthogonal biaxial strain gauge (KFGS-1-120-D16-11, Kyowa Electric, Tokyo, Japan) with a gauge length of 2.0 mm was attached to the center of the specimen, and a four-point bending test was performed on the surface to which the gauge was attached. The bending test involved an adhesion evaluation device (DTS, Nissan Arc, Yokosuka, Japan) under the following conditions: an upper fulcrum distance of 12 mm, lower fulcrum distance of 22 mm, and crosshead speed of 2.0 μm/min under a 37 °C environment (considering the oral cavity). The elastic modulus was calculated based on the slope of the obtained stress–strain curve, and the Poisson's ratio was calculated from the ratio of the bending strain to the lateral strain (n = 5).

2.5. Chemical composition and microstructural observation

Chemical composition analyses were performed via X-ray diffraction (XRD), with Cu Kα radiation at 30 kV and 15 mA, and X-ray fluorescence (XRF) analysis. XRD analysis was performed on the sintered specimens along each building direction using a desktop X-ray diffractometer (MiniFlex, Rigaku, Tokyo, Japan) (n = 6). XRF was performed using a fluorescent X-ray analyzer (DELTA Professional, OLYMPUS, Tokyo, Japan). The microstructures were observed via scanning electron microscopy (SEM) (JSM-IT200, JEOL, Tokyo, Japan) at an accelerating voltage of 15.0 kV, after sputter-coating the specimens with platinum under an argon gas environment using a sputter-coater machine (E-1030, Hitachi, Tokyo, Japan).

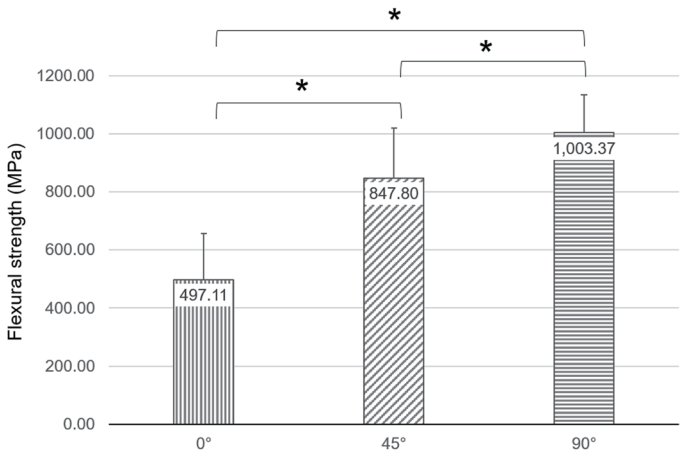

Fig. 2. Flexural strength of additive-manufactured zirconia specimens. 0°: parallel; 45°: diagonal; 90°: perpendicular. * Statistically significant differences between marked groups (α = 0.05).

2.6. Statistical analyses

The normality of the data distribution and homogeneity of variance for the measured flexural strength, Vickers hardness, fracture toughness, and elastic modulus were first verified using the Shapiro-Wilk test and Levene's test, respectively. When the results of Levene's test revealed the equality of variances, a one-way analysis of variance and Tukey's honestly significant difference test were performed. If the results of Levene's test did not show homogeneity, nonparametric procedures were used (i.e., the Kruskal-Wallis test and the Steel-Dwass multiple comparison test). The statistical significance level was set at 5%. All statistical tests were performed using statistical software (IBM SPSS Statistics 24, IBM, Armonk, NY, USA).

3. Results

Post-hoc power analysis was performed before the statistical analyses, which revealed that the values of power were larger than 0.8 in all results. Both Kolmogorov-Smirnov and Levene's test results of the flexural strength, Vickers hardness, fracture toughness, and elastic modulus yielded p-values greater than 0.05. The results were analyzed using a one-way analysis of variance and Tukey's honestly significant difference test.

3.1. Flexural strength

The flexural strengths measured along each tested direction are shown in **Figure 2**. The highest flexural strength was obtained when the building direction was perpendicular to the fabrication direction. Notably, statistical analyses revealed significant differences between the flexural strengths obtained along all directions (p = 0.00, post-

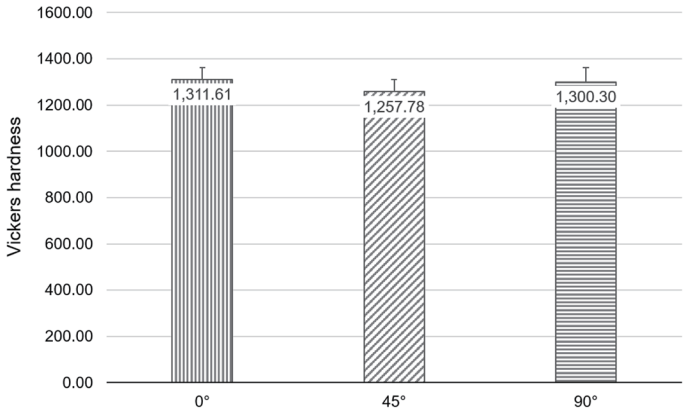

Fig. 3. Vickers hardness of additive-manufactured zirconia specimens. 0°: parallel, 45°: diagonal, 90°: perpendicular.

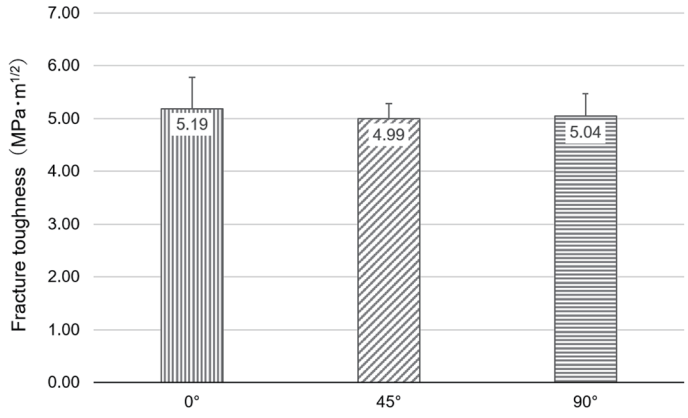

Fig. 4. Fracture toughness of additive-manufactured zirconia specimens. 0°: parallel, 45°: diagonal, 90°: perpendicular.

hoc power = 0.99).

3.2. Vickers hardness and fracture toughness

The Vickers hardness and fracture toughness results are shown in **Figures 3 and 4**, respectively. The Vickers hardness and fracture toughness of the specimens were similar in the three different directions, thereby revealing no significant differences between the building directions (Vickers hardness: $p = 0.09$, post-hoc power = 0.84; fracture toughness: $p = 0.61$, post-hoc power = 0.80).

3.3. Elastic modulus and Poisson's ratio

The elastic moduli of each group are listed in **Table 2**. The highest elastic modulus was observed in the perpendicular direction; elastic moduli of 187.67 and 187.33 GPa were obtained along the Y- and X-axes, respectively. However, no significant difference was noted in the measured values along the different fabrication directions ($p = 0.22$, post-hoc power = 1.00). The Poisson's ratios are listed in **Table 2**. The results show that the measured values for the specimens along the three directions were similar, and there was no significant difference with respect to the building direction ($p = 0.19$, post-hoc power = 0.83).

Table 2. Results for elastic modulus and Poisson's ratio (n = 5)

	0 °	45 °	90°-x	90°-y
Elastic modulus	173.33 (±4.51)	179.67 (±2.31)	187.33 (±2.52)	187.67 (±3.06)
Poisson's ratio	0.33 (±0.01)	0.32 (±0.01)	0.32 (±0.01)	0.33 (±0.01)

0°: parallel, 45°: diagonal, 90°: perpendicular directions, 90°-x, 90°-y: horizontal to the building stage

3.4. Chemical composition and microstructural analysis

The XRF results are listed in **Table 3**. The chemical-component analysis of the specimens shows that almost no change was observed with respect to the building direction. The XRD spectra of the zirconia specimens along the three dimensions are shown in **Figure 5**. The peak intensities in the XRD patterns were different for each spectrum. Characteristic reflections were observed between 31° and 32° in 2θ for each direction. The XRD patterns of all specimens indicated the presence of the tetragonal phase. There was no difference in the diffraction angles of the peaks that showed the standard pattern for sintered Y-TZP with respect to the building direction for each zirconia specimen. Typical surface-structure images for different directions of the zirconia specimens are shown in **Figure 6**. At 100× magnification, a large number of small voids aligned perpendicular to the building direction were observed in the 0 °direction, and layers with a spacing of approximately 30 μm were identified. No layers and only a few voids were observed in the 45 °and 90 °directions. At 5000× magnification, a lower density of large crystals with many porous voids was observed in the 0°direction compared with those for the 45° and 90° directions. Among the three directions, the 0°-direction specimens exhibited similar microstructures in terms of grain size and phase composition, and critical defects were observed.

4. Discussion

The main goal of this study is to compare the mechanical properties of SLA-manufactured zirconia materials for different building directions. Based on these results, the null hypothesis was partially rejected. The experimental results revealed that the mechanical properties of the SLA-manufactured zirconia specimens, in particular, the flexural strength, were affected by the building direction. However, the Vickers hardness, fracture toughness, elastic modulus, and Poisson's ratio remained unaffected. The highest flexural strength was observed when the building direction was 90°, followed by that at 45°, and the smallest difference between the conditions was observed at 0°. Based on the flexural-strength test results, the strength of the SLA-manufactured zirconia specimens tended to be lower than that of previously reported subtractive-manufactured zirconia specimens regardless of the building direction[39]. Although a comparison with SM technology was not conducted in this study, other studies comparing AM and SM technologies reported that SLA- and DLP-manufactured zirconia specimens tended to exhibit lower flexural strengths than subtractive-manufactured zirconia specimens[35,40]. Additionally, specimens in which the building and loading directions are parallel exhibit lower flexural strengths than those loaded perpendicular to the building direction[33]. According to the study by Marisco et al.[33], in the flexural-strength test of DLP-manufactured zirconia specimens, the strength was the lowest when the building direction and load direction were parallel, and the strength tended to increase from the diagonal direction to the vertical direction. In this study, the fracture surface was almost parallel to

Table 3. Chemical analysis of the different specimens tested in this study in terms of oxides, as measured via XRF (n = 6)

	Zr	S	Si	Hf	Al	Nb	Sb	Pd	Cd
0 ˚	82.46 (1.61)	5.38 (034)	4.92 (0.23)	1.95 (0.07)	3.83 (1.70)	0.82 (0.01)	0.24 (0.05)	0.22 (0.02)	0.21 (0.02)
45 ˚	84.22 (2.23)	5.81 (1.18)	5.21 (0.95)	4.84 (6.99)	1.13 (0.28)	0.84 (0.22)	0.25 (0.03)	0.22 (0.01)	0.22 (0.02)
90°	83.02 (1.08)	6.34 (0.41)	5.69 (0.47)	1.95 (0.06)	1.57 (0.33)	0.83 (0.02)	0.22 (0.01)	0.21 (0.02)	0.21 (0.02)

In parentheses indicates wt%
0°: parallel, 45°: diagonal, 90°: perpendicular directions

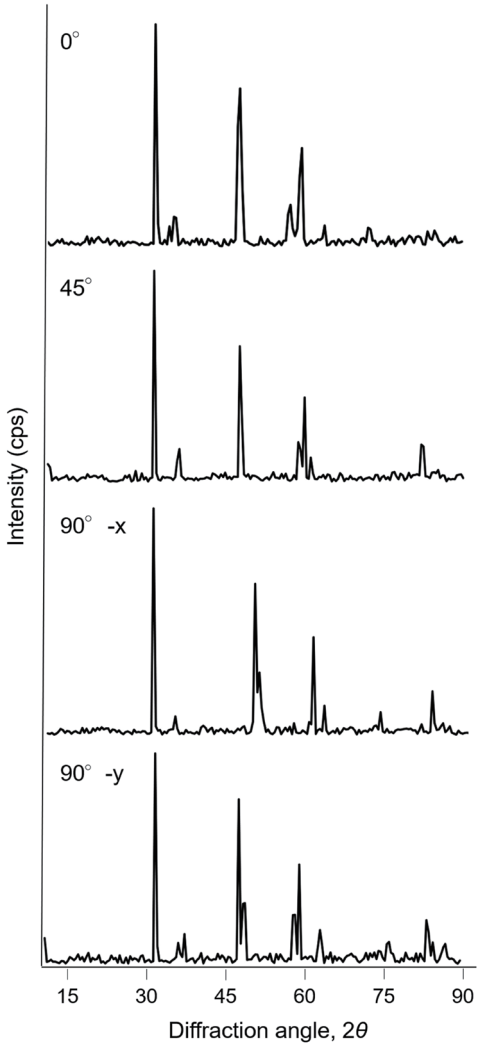

Fig. 5. XRD spectra for the 0°, 45°, 90°-x, and 90°-y specimens.

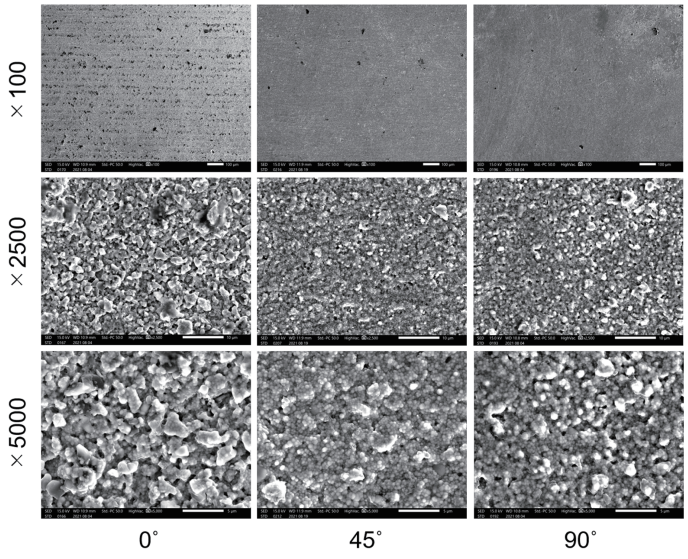

Fig. 6. SEM images of the 0°, 45°, and 90° specimens. top: 100× magnification; middle: 2500× magnification; bottom: 5000× magnification.

the layer boundaries for specimens built in the 0° direction; therefore, cracks could easily propagate along them. The specimen constructed perpendicular to the load exhibited the highest strength. Moreover, microstructural analyses revealed that layers, large crystals, and pores were more prominent in the 0° direction. Notably, more layers were observed at 0° and 45° than at 90°, thereby resulting in additional layer boundaries. Therefore, it can be concluded that layer boundaries have a particular effect on the anisotropic behavior of the builds. Zandinejad et al.[41] reported the flexural strength of 3 mol% yttria-stabilized additive-manufactured zirconia specimens according to porosity. They prepared specimens with 0%, 20%, and 40% porosities and conducted three-point bending tests. Their results showed that the flexural strength of the specimens with 20% porosity was almost half of that of the specimens with 0% porosity. However, in this study, the flexural strength of the 0° specimens was half that of the 90° specimens. Based on the abovementioned study, it is suggested that the 90° specimens had a 20% larger porosity than the 0° specimens.

The measured Vickers-hardness and fracture-toughness values of the SLA-manufactured zirconia specimens did not exhibit any significant differences with respect to the building direction. It has been reported that the Vickers hardness of DLP-manufactured zirconia specimens is approximately 5% lower than that of subtractive-manufactured specimens, whereas the fracture toughness values are almost identical[29]. Furthermore, Marsico et al.[33] reported no significant differences in the Vickers hardness of DLP-manufactured zirconia specimens according to the building direction. Thus, our findings are in agreement with other reported measurements for stabilized zirconia. Therefore, it can be concluded that its hardness is almost equal to that of zirconia obtained using SM technology[29]. However, a comparison of the fracture toughness along different building directions for DLP-manufactured zirconia specimens showed that the 45° direction affords a significantly higher indentation fracture toughness than other orientations[33]. Previous studies have reported that differences in the K_{IC} values for zirconia may be

due to differences in empirical formulas[29]. No definitive conclusions have been reported; however, it is worth noting that certain researchers believe that indentation-fracture toughness is controversial and unsuitable for true fracture-toughness (K_{IC}) measurements. Nevertheless, if the test configuration is consistent, the consistency of the measurement approach can be useful for comparative measurements of the fracture resistance (*Kc*)[33,42].

There was no significant difference in the measured elastic modulus with respect to the building direction. For different building directions, the elastic modulus of DLP-manufactured zirconia specimens was reported to be 191–218 GPa, which is consistent with the elastic modulus of subtractive-manufactured specimens (200–220 GPa)[33]. However, the measured values for the SLA-manufactured zirconia specimens in this study were smaller than those for the stabilized zirconia specimens. Thus, the low elastic modulus of the SLA-manufactured zirconia specimens may be attributed to the difference in the method used (i.e., DLP). Furthermore, in the DLP-manufactured zirconia specimens, there was a significant difference in the elastic modulus, depending on the building direction. This difference can be attributed to the layer-line and layer-plane orientations, which were perpendicular to the plane of the maximum normal stress[33]. It has also been reported that the elastic modulus and Poisson's ratio of zirconia ceramics decrease with increasing pore-space volume[43]. Thus, the factors that affect the mechanical properties of SLA-manufactured zirconia specimens are not only affected by the building direction, but also by the apparatus and manufacturing process (from additive manufacturing to sintering).

Based on XRD phase analyses, this study demonstrates that SLA-manufactured zirconia specimens exhibit comparable chemical compositions regardless of the building direction. Similar XRD patterns have been reported for additive- and subtractive-manufactured zirconia specimens[29,44]. Our results are similar to those of previous reports. Some heavy metals were observed in all the specimens as minor constituents. These elements were also observed in zirconia dental implants; notably, heavy metals were likely introduced by contamination during the purification and production processes[45]. However, the biological significance of this has not yet been investigated, and the minor constituents may affect the chemical, mechanical, and surface properties of the implants, thereby changing their clinical behavior[46]. However, an existing concern is that additively manufactured zirconia is considered to possess a higher residual porosity, owing to the layer-by-layer production method. In DLP-manufactured zirconia specimens, the mechanism responsible for building-direction dependencies has been attributed to incomplete coupling between successive building layers[33]. The most common solution that can help minimize imperfect layer binding is to reduce the layer height. This promotes more effective sintering across the layers, and the parts printed at lower layer heights exhibit no evidence of layer lines or associated defects in the microstructure of the final sintered part. However, previous studies show that reducing the layer height significantly increases the required building time, which makes fabrication difficult[33,47]. According to Galante et al.[15], the accuracy in the Z-direction is typically worse and more difficult to improve than that in the X- and Y-directions because it is influenced by a variety of process parameters that are difficult to control. Additionally, the resolution in the Z-direction, which is determined by the curing depth in each layer, is more critical and is controlled by the amount of photoinitiators, particle size and shape, and exposure variables such as wavelength, laser power, beam size and speed, and exposure time and velocity[48,49]. Furthermore, the curing depth is a critical parameter that determines the formability accuracy. If photocuring is not sufficiently deep, delamination between layers may occur, thereby leading to defects that can significantly affect the physical properties of the sintered products[50]. De-binding is also an important parameter. If the removal rate of volatile products resulting from the decomposition of the binder is too high, the pressure will increase, which may cause crack formation and delamination. Therefore, the de-binding temperature should be carefully selected[15].

Wang et al.[28] mentioned that owing to the surface-stepping phenomenon in 3D printing, occlusal surfaces or large curved surfaces are more error-prone than vertical surfaces, which adversely affects the trueness of the crowns in larger grooves and line-angle areas. Anisotropy and residual stresses should be eliminated, owing to the complex structure of dental prostheses and various stress directions during mastication. Thus, solutions that improve the accuracy of different building directions, compensate for sintering shrinkage, and reduce porosity are essential to ensure the reliable use of manufactured dental prostheses[15]. Previous studies show that the surface roughness of monolithic additive-manufactured zirconia crowns is lower than that of subtractive-manufactured crowns; therefore, it demonstrates excellent surface properties[51]. Surface quality is an important factor because mechanical properties are affected by the presence of defects in terms of occlusal attrition. SLA-manufactured zirconia crowns feature an excellent surface finish, thereby shortening the time required for polishing.

AM technology is recognized as a promising technology that offers advantages not only in the production of customized prostheses to improve health and quality of life but also in terms of its ability to decrease environmental impacts and enhance manufacturing sustainability[15]. However, porosity control and sintering distortion remain unaddressed challenges because most AM technologies that utilize zirconia materials require post-printing sintering processes[15,52]. Furthermore, AM technology does not offer a significant advantage in terms of production speed compared to SM technology. SLA-manufactured specimens require longer post-processing times[15]. AM printing requires half a day for cleaning, seven days for degreasing, and two days for sintering (following the manufacturer's instructions). Furthermore, zirconia materials used in AM technology for dental prostheses are currently only available in white, and their opacity may compromise esthetic features[15]. Tooth color is another challenge that hinders the successful application and development of this technology in dentistry. In the future, reduced material and equipment costs, improved accuracy, and the development of appropriate tooth colors will make this technology suitable for clinical practice. Achieving this requires further studies that consider the effects of building direction, manufacturing protocol, occlusal anatomy, and coloring methods, as well as establish a standard fabrication method.

5. Conclusions

Within the limits of this study (e.g., *in vitro* design, number of specimens evaluated, only one material and apparatus used), the flexural strength was observed to be influenced by the building direction in SLA-manufactured zirconia specimens. The highest flexural strength was obtained when the building direction was perpendicular to the fabrication direction. The fracture toughness, elastic modulus, Poisson's ratio, and chemical composition remained unaffected, and there were no significant differences in these prop-

erties between the building directions. Microstructural observations revealed that layers, large crystals, and pores were more prominent when the building direction was parallel to the fabrication direction. The layer boundaries were considered to affect the anisotropic behavior of the builds to a certain extent, owing to the layer-by-layer production method. It is possible that these mechanical properties are affected not only by the building direction, but also by differences in the AM method (e.g., manufacturing method, curing depth, de-binder temperature, porosity, and sintering shrinkage). AM technology is still premature for clinical application and requires further *in vitro* testing to determine its basic mechanical, physical, and optical properties. Moreover, further *in vivo* testing is required based on these assessments.

Funding

This work was supported by a Grant-in-Aid for Scientific Research (C:21K10026) from the Japan Society for the Promotion of Science and Miyata Research Grant A.

Conflicts of Interest

The authors declare that they have no conflicts of interest.

References

[1] Blatz MB, Chiche G, Bahat O, Roblee R, Coachman C, Heymann HO. Evolution of Aesthetic Dentistry. J Dent Res. 2019;98:1294–304. https://doi.org/10.1177/0022034519875450, PMID:31633462

[2] Miura S, Tsukada S, Fujita T, Isogai T, Teshigawara D, Saito-Murakami K, *et al.* Effects of abutment tooth and luting agent colors on final color of high-translucent zirconia crowns. J Prosthodont Res. 2022;66:243–9. https://doi.org/10.2186/jpr.JPR_D_21_00025, PMID:34321374

[3] Lerner H, Nagy K, Pranno N, Zarone F, Admakin O, Mangano F. Trueness and precision of 3D-printed versus milled monolithic zirconia crowns: an in vitro study. J Dent. 2021;113:103792. https://doi.org/10.1016/j.jdent.2021.103792, PMID:34481929

[4] Sailer I, Balmer M, Hüsler J, Hämmerle CHF, Känel S, Thoma DS. 10-year randomized trial (RCT) of zirconia-ceramic and metal-ceramic fixed dental prostheses. J Dent. 2018;76:32–9. https://doi.org/10.1016/j.jdent.2018.05.015, PMID:29807060

[5] Miura S, Kasahara S, Yamauchi S, Okuyama Y, Izumida A, Aida J, *et al.* Clinical evaluation of zirconia-based all-ceramic single crowns: an up to 12-year retrospective cohort study. Clin Oral Investig. 2018;22:697–706. https://doi.org/10.1007/s00784-017-2142-y, PMID:28608051

[6] Miura S, Yamauchi S, Kasahara S, Katsuda Y, Fujisawa M, Egusa H. Clinical evaluation of monolithic zirconia crowns: a failure analysis of clinically obtained cases from a 3.5-year study. J Prosthodont Res. 2021;65:148–54. https://doi.org/10.2186/jpr.JPOR_2019_643, PMID:32938882

[7] Solá-Ruiz MF, Baixauli-López M, Roig-Vanaclocha A, Amengual-Lorenzo J, Agustín-Panadero R. Prospective study of monolithic zirconia crowns: clinical behavior and survival rate at a 5-year follow-up. J Prosthodont Res. 2021;65:284–90. https://doi.org/10.2186/jpr.JPR_D_20_00034, PMID:33041280

[8] Silva NRFA, Witek L, Coelho PG, Thompson VP, Rekow ED, Smay J. Additive CAD/CAM process for dental prostheses. J Prosthodont. 2011;20:93–6. https://doi.org/10.1111/j.1532-849X.2010.00623.x, PMID:20561158

[9] Tan X, Zhao Y, Lu Y, Yu P, Mei Z, Yu H. Physical and biological implications of accelerated aging on stereolithographic additive-manufactured zirconia for dental implant abutment. J Prosthodont Res. 2021;66:600–9. https://doi.org/10.2186/jpr.JPR_D_21_00240, PMID:34924492

[10] Harada K, Shinya A, Yokoyama D, Shinya A. Effect of loading conditions on the fracture toughness of zirconia. J Prosthodont Res. 2013;57:82–7. https://doi.org/10.1016/j.jpor.2013.01.005, PMID:23498598

[11] Miyazaki T, Nakamura T, Matsumura H, Ban S, Kobayashi T. Current status of zirconia restoration. J Prosthodont Res. 2013;57:236–61. https://doi.org/10.1016/j.jpor.2013.09.001, PMID:24140561

[12] Rosentritt M, Preis V, Behr M, Strasser T. Fatigue and wear behaviour of zirconia materials. J Mech Behav Biomed Mater. 2020;110:103970. https://doi.org/10.1016/j.jmbbm.2020.103970, PMID:32957257

[13] Okazaki Y, Ishino A. Microstructures and Mechanical Properties of Laser-Sintered Commercially Pure Ti and Ti-6Al-4V Alloy for Dental Applications. Materials (Basel). 2020;13:609. https://doi.org/10.3390/ma13030609, PMID:32013199

[14] van Noort R. The future of dental devices is digital. Dent Mater. 2012;28:3–12. https://doi.org/10.1016/j.dental.2011.10.014, PMID:22119539

[15] Galante R, Figueiredo-Pina CG, Serro AP. Additive manufacturing of ceramics for dental applications: A review. Dent Mater. 2019;35:825–46. https://doi.org/10.1016/j.dental.2019.02.026, PMID:30948230

[16] Additive manufacturing -General principles- Terminology. ISO/ASTM 52900. 2021.

[17] Ligon SC, Liska R, Stampfl J, Gurr M, Mülhaupt R. Polymers for 3D Printing and Customized Additive Manufacturing. Chem Rev. 2017;117:10212–90. https://doi.org/10.1021/acs.chemrev.7b00074, PMID:28756658

[18] Salmi M. Additive Manufacturing Processes in Medical Applications. Materials (Basel). 2021;14:191. https://doi.org/10.3390/ma14010191, PMID:33401601

[19] Javaid M, Haleem A. Current status and applications of additive manufacturing in dentistry: A literature-based review. J Oral Biol Craniofac Res. 2019;9:179–85. https://doi.org/10.1016/j.jobcr.2019.04.004, PMID:31049281

[20] Sulaiman TA. Materials in digital dentistry—A review. J Esthet Restor Dent. 2020;32:171–81. https://doi.org/10.1111/jerd.12566, PMID:31943720

[21] Tamac E, Toksavul S, Toman M. Clinical marginal and internal adaptation of CAD/CAM milling, laser sintering, and cast metal ceramic crowns. J Prosthet Dent. 2014;112:909–13. https://doi.org/10.1016/j.prosdent.2013.12.020, PMID:24819532

[22] Kajima Y, Takaichi A, Nakamoto T, Kimura T, Yogo Y, Ashida M, *et al.* Fatigue strength of Co–Cr–Mo alloy clasps prepared by selective laser melting. J Mech Behav Biomed Mater. 2016;59:446–58. https://doi.org/10.1016/j.jmbbm.2016.02.032, PMID:26974490

[23] Konieczny B, Szczesio-Wlodarczyk A, Sokolowski J, Bociong K. Challenges of Co–Cr Alloy Additive Manufacturing Methods in Dentistry—The Current State of Knowledge (Systematic Review). Materials (Basel). 2020;13:3524. https://doi.org/10.3390/ma13163524, PMID:32785055

[24] Kanazawa M, Iwaki M, Minakuchi S, Nomura N. Fabrication of titanium alloy frameworks for complete dentures by selective laser melting. J Prosthet Dent. 2014;112:1441–7. https://doi.org/10.1016/j.prosdent.2014.06.017, PMID:25258261

[25] Huang Z, Zhang L, Zhu J, Zhang X. Clinical marginal and internal fit of metal ceramic crowns fabricated with a selective laser melting technology. J Prosthet Dent. 2015;113:623–7. https://doi.org/10.1016/j.prosdent.2014.10.012, PMID:25794918

[26] Sancho-Puchades M, Fehmer V, Hämmerle C, Sailer I. Advanced smile diagnostics using CAD/CAM mock-ups. Int J Esthet Dent. 2015;10:374–91. PMID:26171442

[27] Oliveira TT, Reis AC. Fabrication of dental implants by the additive manufacturing method: A systematic review. J Prosthet Dent. 2019;122:270–4. https://doi.org/10.1016/j.prosdent.2019.01.018, PMID:30928226

[28] Wang W, Yu H, Liu Y, Jiang X, Gao B. Trueness analysis of zirconia crowns fabricated with 3-dimensional printing. J Prosthet Dent. 2019;121:285–91. https://doi.org/10.1016/j.prosdent.2018.04.012, PMID:30017167

[29] Mei Z, Lu Y, Lou Y, Yu P, Sun M, Tan X, *et al.* Determination of Hardness and Fracture Toughness of Y-TZP Manufactured by Digital Light Processing through the Indentation Technique. BioMed Res Int. 2021;2021:1–11. https://doi.org/10.1155/2021/6612840, PMID:33628793

[30] Lu Y, Mei Z, Lou Y, Yue L, Chen X, Sun J, *et al.* Schwickerath adhesion tests of porcelain veneer and stereolithographic additive-manufactured zirconia. Ceram Int. 2020;46:16572–7. https://doi.org/10.1016/j.ceramint.2020.03.228

[31] Methani MM, Revilla-León M, Zandinejad A. The potential of additive manufacturing technologies and their processing parameters for the fabrication of all-ceramic crowns: A review. J Esthet Restor Dent. 2020;32:182–92. https://doi.org/10.1111/jerd.12535, PMID:31701629

[32] Zandinejad A, Methani MM, Schneiderman ED, Revilla-León M, Bds DM. Fracture Resistance of Additively Manufactured Zirconia Crowns when Cemented to Implant Supported Zirconia Abutments: an in vitro Study. J Prosthodont. 2019;28:893–7. https://doi.org/10.1111/jopr.13103, PMID:31430001

[33] Marsico C, Øilo M, Kutsch J, Kauf M, Arola D. Vat polymerization-printed partially stabilized zirconia: mechanical properties, reliability and structural defects. Addit Manuf. 2020;36:101450. https://doi.org/10.1016/j.addma.2020.101450, PMID:32793425

[34] Harada Y, Ishida Y, Miura D, Watanabe S, Aoki H, Miyasaka T, *et al.* Mechanical Properties of Selective Laser Sintering Pure Titanium and Ti-6Al-4V, and Its Anisotropy. Materials (Basel). 2020;13:5081. https://doi.org/10.3390/ma13225081, PMID:33187166

[35] Revilla-León M, Al-Haj Husain N, Ceballos L, Özcan M. Flexural strength and Weibull characteristics of stereolithography additive manufactured versus milled zirconia. J Prosthet Dent. 2021;125:685–90. https://doi.org/10.1016/j.prosdent.2020.01.019, PMID:32434662

[36] Zakeri S, Vippola M, Levänen E. A comprehensive review of the photopolymerization of ceramic resins used in stereolithography. Addit Manuf. 2020;35:101177. https://doi.org/10.1016/j.addma.2020.101177

[37] International Organization for Standardization. Dentistry-Ceramic materials.ISO standard 6872:2015. Geneva: 2015.

[38] Niihara K, Morena R, Hasselman DPH. Evaluation ofK Ic of brittle solids by the indentation method with low crack-to-indent ratios. J Mater Sci Lett. 1982;1:13–6. https://doi.org/10.1007/BF00724706

[39] Hjerppe J, Närhi TO, Vallittu PK, Lassila LVJ. Surface roughness and the flexural and bend strength of zirconia after different surface treatments. J Prosthet Dent. 2016;116:577–83. https://doi.org/10.1016/j.prosdent.2016.02.018, PMID:27157604

[40] Bergler M, Korostoff J, Torrecillas-Martinez L, Mante F. Ceramic Printing—Comparative Study of the Flexural Strength of 3D-Printed and Milled Zirconia. Int J Prosthodont. 2021; Online ahead of print. https://doi.org/10.11607/ijp.6749, PMID:33616569

[41] Zandinejad A, Das O, Barmak AB, Kuttolamadom M, Revilla-Leon M. The Flexural Strength and Flexural Modulus of Stereolithography Additively Manufactured Zirconia with Different Porosities. J Prosthodont. 2021; Online ahead of print. https://doi.org/10.1111/jopr.13430, PMID:34580962

[42] Kruzic JJ, Kim DK, Koester KJ, Ritchie RO. Indentation techniques for evaluating the fracture toughness of biomaterials and hard tissues. J Mech Behav Biomed Mater. 2009;2:384–95. https://doi.org/10.1016/j.jmbbm.2008.10.008, PMID:19627845

[43] Savchenko N, Sevostyanova I, Sablina T, Gömze L, Kulkov S. The influence of porosity on the elasticity and strength of alumina and zirconia. AIP Conf Proc. 2014;1623:547–50. https://doi.org/10.1063/1.4899003

[44] Nakai H, Inokoshi M, Nozaki K, Komatsu K, Kamijo S, Liu H, *et al.* Additively Manufactured Zirconia for Dental Applications. Materials (Basel). 2021;14:3694. https://doi.org/10.3390/ma14133694, PMID:34279264

[45] Gross C, Bergfeldt T, Fretwurst T, Rothweiler R, Nelson K, Stricker A. Elemental analysis of commercial zirconia dental implants - Is "metal-free" devoid of metals? J Mech Behav Biomed Mater. 2020;107:103759. https://doi.org/10.1016/j.jmbbm.2020.103759, PMID:32364951

[46] Preoteasa EA, Ciortea C, Constantinescu B, Fluerasu D, Enescu SE, Pantelica D, *et al.* Analysis of composites for restorative dentistry by PIXE, XRF and ERDA. Nucl Instrum Methods Phys Res B. 2002;189:426–30. https://doi.org/10.1016/S0168-583X(01)01119-3

[47] Xing H, Wu J, Zhou L, Yang S. Natural teeth-retained splint based on a patient-specific 3D-printed mandible used for implant surgery and vestibuloplasty. Medicine (Baltimore). 2017;96:e8812. https://doi.org/10.1097/MD.0000000000008812, PMID:29310359

[48] Melchels FPW, Feijen J, Grijpma DW. A review on stereolithography and its applications in biomedical engineering. Biomaterials. 2010;31:6121–30. https://doi.org/10.1016/j.biomaterials.2010.04.050, PMID:20478613

[49] Stansbury JW, Idacavage MJ. 3D printing with polymers: challenges among expanding options and opportunities. Dent Mater. 2016;32:54–64. https://doi.org/10.1016/j.dental.2015.09.018, PMID:26494268

[50] Jang KJ, Kang JH, Fisher JG, Park SW. Effect of the volume fraction of zirconia suspensions on the microstructure and physical properties of products produced by additive manufacturing. Dent Mater. 2019;35:e97–106. https://doi.org/10.1016/j.dental.2019.02.001, PMID:30833011

[51] Miura S, Fujita T, Tsukada S, Teshigawra D, Saito-Murakami K, Fujisawa M. Comparative Evaluation of the Reproductive Trueness of Zirconia Crowns Fabricated Using Additive Manufacturing and Conventional Milling. Int J Prosthodont. 2022;35:410–3. https://doi.org/10.11607/ijp.7092, PMID:33651036

[52] Revilla-León M, Meyer MJ, Zandinejad A, Özcan M. Additive manufacturing technologies for processing zirconia in dental applications. Int J Comput Dent. 2020;23:27–37. PMID:32207459